

Enhanced ferroelectric and dielectric properties of BiFeO₃–PbTiO₃ thin films grown via a sol–gel multilayer deposition method

Haimin Li¹ · Jianguo Zhu² · Jia Zhuang¹ · Yu Hu¹ · Mingzhe Huai¹ · Qingsong Yang¹

Received: 29 January 2015 / Accepted: 3 April 2015 / Published online: 11 April 2015
© Springer Science+Business Media New York 2015

Abstract BiFeO₃–PbTiO₃ (BF–PT) solid solution thin films were deposited on LaNiO₃/SiO₂/Si substrates by a sol–gel multilayer deposition method in a super clean room with rapid thermal annealing (RTA) technique. XRD patterns of all the films demonstrate a single perovskite phase. The induced orientation of LaNiO₃ substrates leads to highly (100) oriented texture. Cross-section SEM and EDS pictures confirmed that the BFPT-based films are about 230 nm thickness and had formed a dense and uniform solid solution. Film with a ratio of BF:PT = 1:2 (BFPT1-2) possesses best ferroelectric properties. A saturated hysteresis loop with a remnant polarization of 66 μC/cm² measured at room temperature was obtained, much higher than that of BFPT7030 thin film, which was prepared by depositing BFPT7030 sol directly on LaNiO₃/SiO₂/Si substrates without multilayer deposition. BFPT1-2 thin films also showed better dielectric and leakage current properties than BFPT7030 thin film in the test range of electric field and frequency. BFPT1-2 thin films exhibit lowest leakage current and loss tangent, indicating that a high quality of BFPT1-2 thin film was successfully prepared by multilayer deposition method with a RTA technique with heating rate of 1 °C/s.

Keywords Ferroelectric · BiFeO₃–PbTiO₃ · Multilayer deposition · Sol–gel

1 Introduction

BiFeO₃ is an interesting ferroelectric material which shows very high Curie temperature ($T_C \sim 1103$ K) [1]. High Curie temperature indicates that it possesses high remnant polarization [2]. And the structure of its ferroelectric phase shows huge shifts of Bi³⁺ and Fe³⁺ ions, as well as rotations of oxygen octahedrons along $\langle 111 \rangle$ direction from the nonferroelectric centrosymmetric cubic structure, resulting in the $R3c$ space group and a very high spontaneous electric polarization [3]. Neaton et al. [4] calculated BiFeO₃ has a large ferroelectric polarization of 90–100 μC/cm² with the crystal structure of rhombohedral with space group $R3c$ by using density functional theory within the local spin density approximation method. Although in the past 10 years, people gave numerous attentions on BiFeO₃ [5–9], it is still worth to research because of its obvious advantages and the potential applications as high-density memories, thin film capacitors, actuators and even in new energy devices [10].

BiFeO₃ has a distorted perovskite structure which makes it unstable on structure. In order to improve the ferroelectric performance, different kinds of perovskite structure were introduced to form solid solutions with BiFeO₃ [11–13]. Among them, PbTiO₃ appears to be one of the most promising end materials because the introduction of PbTiO₃ not only stabilizes the perovskite phase but also forms a morphotropic phase boundary (MPB) with BiFeO₃ due to the difference in crystal symmetry between PbTiO₃ and BiFeO₃. The $(1-x)\text{BiFeO}_3-x\text{PbTiO}_3$ (BFPT100x) system has attracted great attention since the system has been suggested to exhibit high ferroelectric performance with an MPB in BFPT100x at the composition of $x \approx 0.3$ [14]. BFPT100x system with different x has been studied carefully to obtain its precise structural details [15–18]. It is found that MPB structure is not only related to the x , but

✉ Haimin Li
luciale@126.com

¹ College of Materials Science and Engineering, Southwest Petroleum University, Chengdu 610500, China

² College of Materials Science and Engineering, Sichuan University, Chengdu 610000, China

also related to its sintered temperature [19]. Very recently, Ashoka [19] have found that the metastable phase is a very common feature in the BFPT100 x system and it affects the ferroelectric properties quite remarkably. MPB structure is beneficial for piezoelectric properties and also, from the data in the literatures, it is beneficial for enhancement of remnant polarization of BFPT100 x solid solution [19, 20]. However, it is hard to find MPB structure in BFPT100 x thin films, most of BFPT100 x thin films exhibit cubic (pseudocubic) or monoclinic phase [21–24], whereas, very recently, Esat et al. [25] have prepared a BFPT7030 thin film by pulsed laser deposition (PLD) method, which showed rhombohedral–tetragonal mixed phase.

BFPT100 x thin films suffered from large leakage mainly due to oxygen vacancies, accompanied by the volatilization of Bi and Pb, which results in difficulty to test out saturated hysteresis loops even in those thin films that are supposed to have MPB structure, i.e., BFPT100 x ($x \approx 3$) thin films [23, 24, 26]. PbTiO₃ showed better insulation resistance and have larger adherence force than BiFeO₃ on substrate, which arouse our interest to prepare BFPT100 x thin films by multilayer deposition method to flexibly adjust the composition and deposition sequence. In this paper, we prepared five BFPT-based thin films by sol–gel multilayer deposition method in a super clean room and obviously enhancement of ferroelectric, dielectric and leakage current properties had been found in these films which can be compared to those high-quality films prepared by pulse laser deposition method [25]. Since BFPT7030 thin films showed better ferroelectric properties than other BFPT100 x thin films prepared by sol–gel method [23, 26], and MPB structure has been found in BFPT7030 bulk and film material [16, 21, 25], therefore, we also prepared a BFPT7030 thin film by directly depositing BFPT7030 sol on the substrates. We found that BFPT-based films prepared by multilayer deposition method showed much higher remnant polarization, lower leakage current, and less tangent than BFPT7030 thin film.

2 Experiment

BFPT-based thin films were deposited on LaNiO₃(LNO)/SiO₂/Si substrates by sol–gel process. 0.3 M BiFeO₃ (BF) sol was prepared by dissolving bismuth nitrate pentahydrate and iron nitrate nonahydrate in acetic acid and ethylene glycol. The solution was then stirred at room temperature for 6 h in aerated environment. 0.3 M PT sol was prepared by dissolving tetrabutyl titanate (stabilized by acetylacetone) and lead acetate trihydrate in ethylene glycol and then stirred at 45 °C for 6 h in aerated environment. Diethanol amine was added to BF and PT sol to increase the viscosity. BFPT7030 sol was also been

prepared; the detailed process has been discussed in our previous work [27]. The depositions were carried out in a super clean room by spin coating at 2500 rpm for 30 s. Five BFPT-based multilayered deposition films of BFPT1-1, BFPT1-2, BFPT1-3, BFPT2-1 and BFPT3-1 were prepared. All the BFPT-based multilayered films contain twelve layers with BF or PT alternatively deposited on the substrates, and in all configurations, the PT layers were deposited before the BF layers. For example, BFPT1-1 was prepared by deposition of 1 layer PT followed by deposition of 1 layer BF and then repeated this circle six times. BFPT1-2 was prepared by deposition of 2 layer PT followed by deposition of 1 layer BF, and then this circle was repeated four times. BFPT7030 thin film was prepared by depositing eight layers of BFPT7030 sol directly on the substrates. Each deposition layer was dried for 1 and 3 min at 150 and 200 °C, respectively, and then annealed at 700 °C for 90 s by rapid thermal annealing (RTA) technique with heating rate of 1 °C/s.

X-ray diffraction (XRD, DX-1000, Dandong, China) with Cu K α radiation ($\lambda = 1.54056 \text{ \AA}$) in the mode of θ – 2θ scan was used for the phase analysis of the films. The cross-section morphology and energy-dispersive spectrometer (EDS) of these films were analyzed using a field-emission scanning electron microscope (FE-SEM, HITACHI S4800, Japan). The ferroelectric properties of the films were measured using Au as top electrodes, which were directly evaporated on the annealed films through a shadow mask with a diameter of 0.5 mm by dc sputtering, forming a Au/BFPT/LNO/SiO₂/Si(100) stacked capacitor. The LaNiO₃ (LNO) layer of the LaNiO₃/SiO₂/Si substrates was used as a bottom electrode. LNO was deposited on SiO₂/Si substrate by rf magnetron sputtering at the substrate temperature of 450 °C with the ratio of oxygen and argon of 10:40 SCCM (SCCM denotes cubic centimeter per minute at STP) under a working pressure of 2.0 Pa. The hysteresis loops of polarization (P) as a function of applied electric field (E) (P – E curve) and leakage current properties of these thin films were evaluated by using the Radiant Precision Ferroelectric Measurement System (RT2000 Tester, USA). The dielectric constant and loss tangent measurement were performed by Agilent 4194A precision impedance analyzer.

3 Results and discussion

Figure 1 shows all the six thin films XRD diffraction patterns in the 2θ range of 20–80. All the films demonstrate single perovskite phase despite different proportion of PT and BF. No individual peaks of PT or BF were found in the five BFPT-based thin films, suggesting intermixing of these films during post-deposition heat treatment and formation

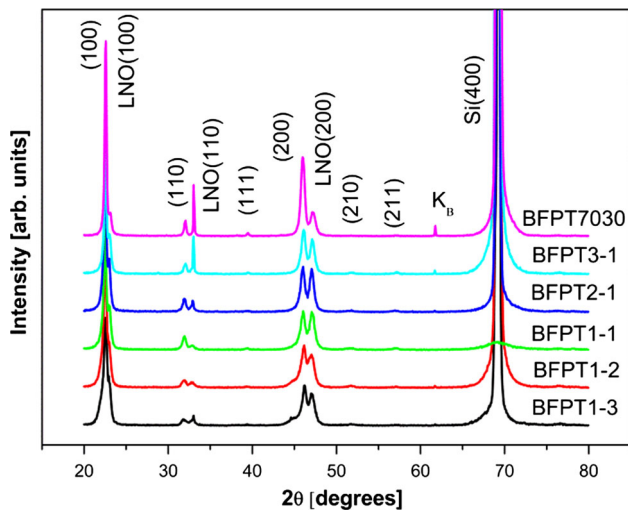


Fig. 1 X-ray diffraction patterns of BFPT1-1, BFPT1-2, BFPT1-3, BFPT2-1, BFPT3-1 and BFPT7030 thin films

of a solid solution. The five BFPT-based thin films prepared by multilayer deposition method show the same diffraction patterns as BFPT7030 thin film, and no peaks were found splitting, indicating that the five BFPT-based thin films have formed a single phase just as BFPT7030 thin film. All the films show highly (100) preferred orientation. The preferential orientation parameter, α_{hkl} , can be calculated by the following formula:

$$\alpha_{hkl} = I_{hkl} / \sum I_{hkl} \quad (1)$$

where I_{hkl} is the relative intensity of the corresponding diffraction peaks. The calculated preferential orientation $\alpha_{(100)}$ of the BFPT1-1, BFPT1-2, BFPT1-3, BFPT2-1, BFPT3-1 and BFPT7030 thin films deposited on LNO/SiO₂/Si substrate is 0.68, 0.70, 0.68, 0.69, 0.68 and 0.67, respectively, indicating that these films are highly (100) oriented with a single perovskite phase, which is quite different from other BFPT100x films deposited on Pt/Si substrates and SiO₂/Si substrates. In this case, the LNO substrate is one of the main attribution to the highly (100) preferred orientation. PbO would also lead to highly (100) preferred orientation [28, 29] since PTO was first deposited on LNO substrate. However, we did not find any PbO peak. And BFPT7030 also showed highly (100) preferred orientation, while it showed highly (110) preferred orientation when deposited on SiO₂/Si substrate [27]. Thus, we figured out that the highly (100) preferred orientation stem from LNO substrate. Wu et al. [30] had confirmed that BiFeO₃ thin films with (100) or (111) preferred orientation would show higher spontaneous polarization and larger fatigue endurance than that of (110) preferred orientation. Thus, in this case, we consider that the highly (100) preferred orientation is beneficial to the ferroelectric and dielectric properties.

To further confirm these films form a solid solution with a single phase instead of multilayer films, the cross-section SEM pictures of BFPT1-1, BFPT1-2 and BFPT2-1 were observed, as shown in Fig. 2. From the SEM pictures, we can see that these films form a solid solution film, no individual layer of BF or PT was observed, which is consistent with the XRD results.

And also, we noticed that the films prepared by multilayer deposition method were less porous and combine more compactly than BFPT7030 films (BF is 0.7 M and PT is 0.3 M, as in our previous work [27]) prepared by sol-gel process deposited directly on SiO₂/Si substrate without multilayer deposition, as shown in Fig. 2. BFPT1-1, BFPT1-2 and BFPT2-1 thin films thickness was about 230 nm, much less than the eight layers BFPT7030 thin film. We consider one of the reasons is that PT layer adheres to the substrates more intensely than BF layer and BFPT7030 layer. In all these multilayered deposition films, BF layer deposited after PT layer deposited on the substrates and it intermixed well with PT layer during post-heat treatment and formed a single phase. It is observed from the pictures that as the BF content increased, the films thickness also increased. We consider, in this case, that BF would form more porous structure, which leads to the increased thickness, and the oxygen vacancies also increased as the porous structure increased and leads to large leakage current.

Figure 3 shows the cross-section EDS results of BFPT1-2 and BFPT2-1 thin films. From the XRD and SEM cross-section pictures, we could not conclude that the films had formed a uniform solid solution although no other phase or individual BF or PT layers were found. To figure out whether the films have formed a uniform structure, we test the cross-section EDS of Bi, Fe, Pb and Ti elements distribution of BFPT1-2 and BFPT2-1 films. Figure 3a shows the Bi, Fe, Pb and Ti distribution in vertical direction of BFPT1-2 film. No obvious distribution difference of these elements in the vertical direction could be found. Figure 3b shows the Bi, Fe, Pb and Ti distribution in the rectangular region, and it can be seen that the four elements are equally distributed. Similarly, no obvious distribution difference of these four elements could be found in the vertical direction or in the rectangular region in BFPT2-1 thin film as seen in Fig. 3c, d.

Thus, we can conclude that although the five BFPT-based thin films were prepared by multilayer deposition method, after subsequent heat treatment, they had formed a uniform solid solution with single phase rather than multilayer structure.

The ferroelectric properties of these films tested at room temperature (RT) are shown in Fig. 4. From the test results, we can see that although BFPT7030 thin film showed a saturated *P*-*E* loop, it showed a much lower *P_r* of 33 μC/

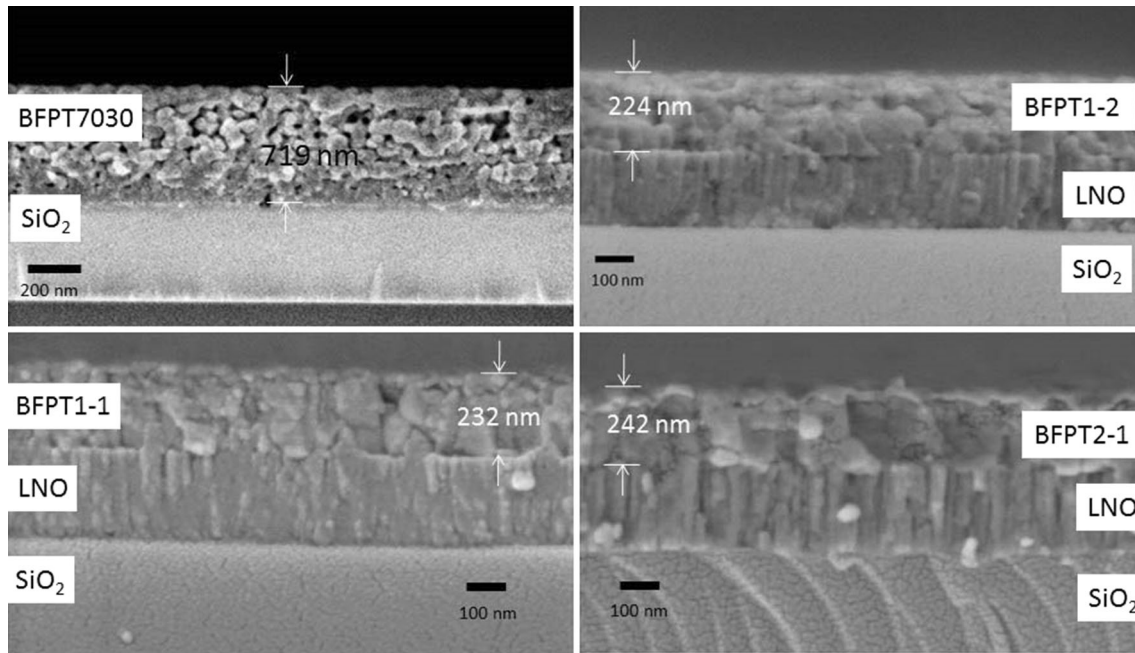


Fig. 2 Cross-section SEM pictures of BFPT1-1, BFPT1-2, BFPT2-1 and BFPT7030 thin films

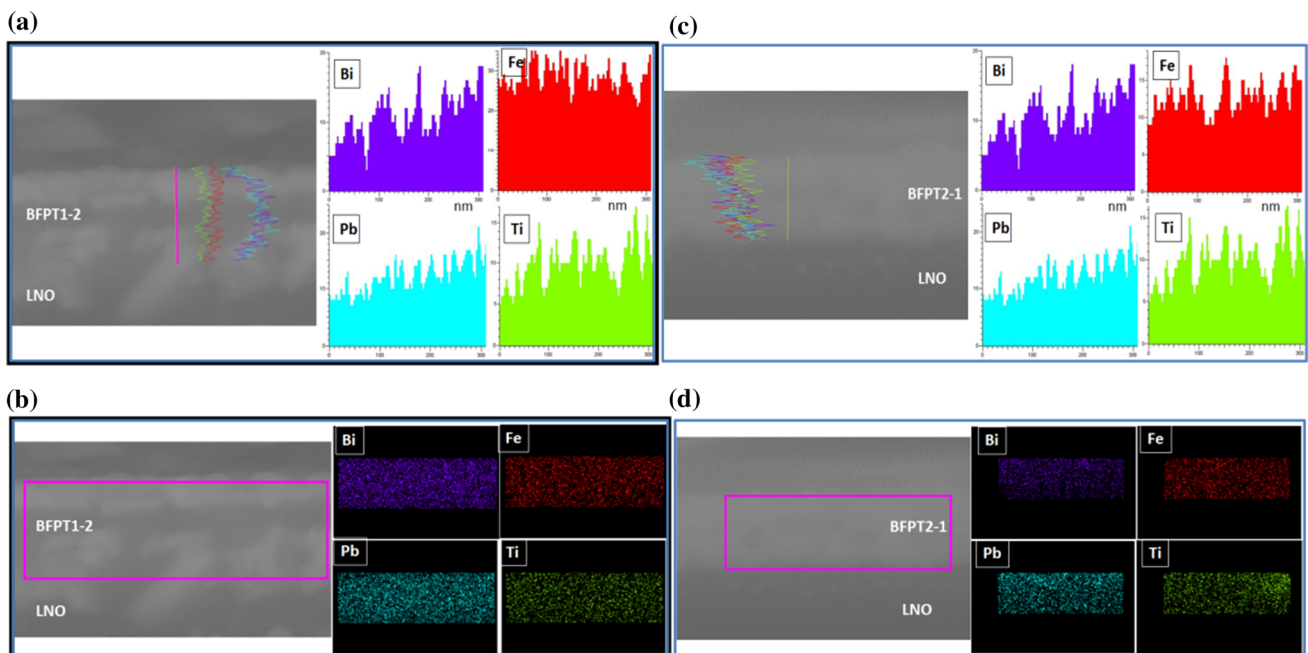


Fig. 3 Cross-section EDS pictures of Bi, Fe, Pb and Ti elements of BFPT1-2 and BFPT2-1 thin films, respectively

cm^2 and a higher E_c of 110 kV/cm than that of BFPT1-2 and BFPT1-3 films. Obviously enhanced ferroelectric properties were found in BFPT1-2 thin film, which showed a saturated hysteresis loop with the highest remnant polarization (P_r) of about $66 \mu\text{C}/\text{cm}^2$, higher than other high-quality BFPT7030 thin films prepared by PLD method [24]. Although high P_r value has also been found in other

BFPT7030 thin film [23], it was measured at a very low temperature (-190°C), which could not get a saturated hysteresis loop at RT, indicating large leakage current in the BFPT7030 thin films, and some other BFPT100x thin films showed rather low P_r prepared by sol-gel process [31] or PLD method [32]. The BFPT1-2 thin film prepared by multilayer deposition method not only shows the

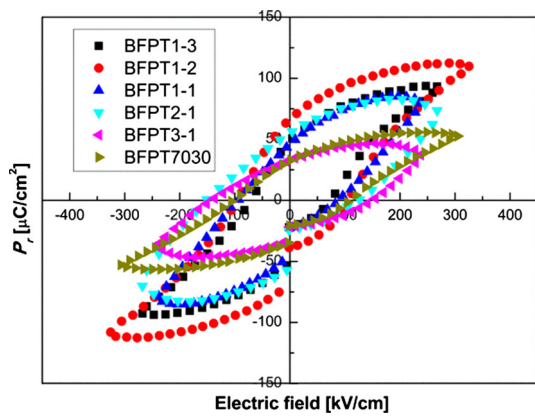


Fig. 4 Room temperature measurement of P - E hysteresis loops of BFPT1-1, BFPT1-2, BFPT1-3, BFPT2-1, BFPT3-1 and BFPT7030 thin films

highest P_r at RT, but also exhibits a low coercive electric field (E_c) of about 100 kV/cm, indicating that it has a high resistance property. BFPT1-3 also shows a saturated hysteresis loop with P_r of about 50 $\mu\text{C}/\text{cm}^2$ and E_c of 75 kV/cm.

However, as BF content increased, the ferroelectric properties decreased. For films of BFPT2-1 and BFPT3-1, no saturated hysteresis loops were found. This is mainly due to that BF had inferior insulation resistance. We ascribe the enhanced ferroelectric properties of BFPT1-2 thin film into four reasons. The first and main reason is that we prepared the films by a multilayer deposition method. By this method, dense and less porous structure thin films were prepared. BF would form more porous structure which results from the hopping electrons from Fe^{3+} to Fe^{2+} and leads to electric conduction. At the same time, oxygen vacancies act as a bridge between Fe^{3+} and Fe^{2+} formed during the variation valence of Fe ions and increase the electric conduction [33]. Since there is little variation valence in PT layer, oxygen vacancies would not form in PT layers and PT could adhere to substrates more dense than BF. By using multilayer deposition method, oxygen vacancies would only exist in BF layers rather than BFPT layers without multilayer deposition method during heat treatment. The second reason is that BFPT1-2 thin film had a proper ratio of BF:PT (1:2), which combine the most advantages of these two materials and form a stable perovskite structure.

The third reason is that we use a rapid thermal annealing (RTA) technique with a heating rate of 1 $^\circ\text{C}/\text{s}$. In our previous work, we found that RTA technique is beneficial to BFPT-based thin films prepared by sol-gel process, which would reduce the volatilization of Bi and Pb ions. And the heating rate of 1 $^\circ\text{C}/\text{s}$ is helpful for getting a better microstructure [27]. And the last reason is that the films

were prepared in a super clean room, which prevents pollution from the air dust or other impurities.

Figure 5 shows the leakage current properties of these six films measured at RT. We test the leakage current of the six films at the same voltage; however, BFPT7030 thin film electric field is lower than other five films, which results from the higher film thickness.

From the test results, it is easy to find that as BF content increased, the leakage current density also increased, which is consistent with the results of ferroelectric hysteresis loops. BFPT1-2 and BFPT1-3 show the lowest leakage current density. However, it is found that the dot lines of leakage current density of BFPT1-2 and BFPT1-3 thin films were more random than other three films; this maybe due to the difference of conduction mechanism of these films. BFPT7030 thin film showed the highest leakage current, which could be ascribed to the more porous structure as shown in Fig. 2.

The relative dielectric constant (ϵ_r) and loss tangent ($\tan\delta$) testing values measured at room temperature are shown in Fig. 6. It was found that BFPT7030 thin film has the largest dielectric constant, ϵ_r is 542 at 1 kHz, and improved dielectric constant can also be found in films of BFPT1-1, BFPT1-2 and BFPT1-3, which is 492, 426 and 434 at 1 kHz, respectively. As the proportion of BF increased, the ϵ_r of the films decreased dramatically. The ϵ_r values are the smallest for the films of BFPT3-1, and it decreased to 217 at 1 kHz, much smaller than that of other films.

Although BFPT7030 showed highest ϵ_r , it showed much higher loss tangent than other films and it increased quickly with increase in frequency. At 1 kHz, $\tan\delta$ of the BFPT7030 film is 0.108. However, BFPT-based films prepared by multilayer deposition method showed much lower loss tangent. When at 1 kHz, $\tan\delta$ of the BFPT3-1 films is 0.06. The $\tan\delta$ value for the films of BFPT1-1 and

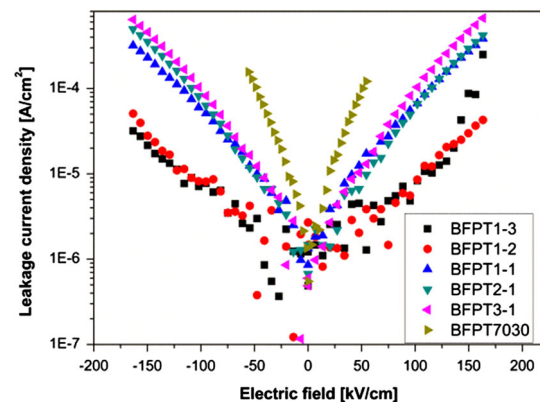


Fig. 5 Leakage current density as a function of electric field of BFPT1-1, BFPT1-2, BFPT1-3, BFPT2-1, BFPT3-1 and BFPT7030 thin films

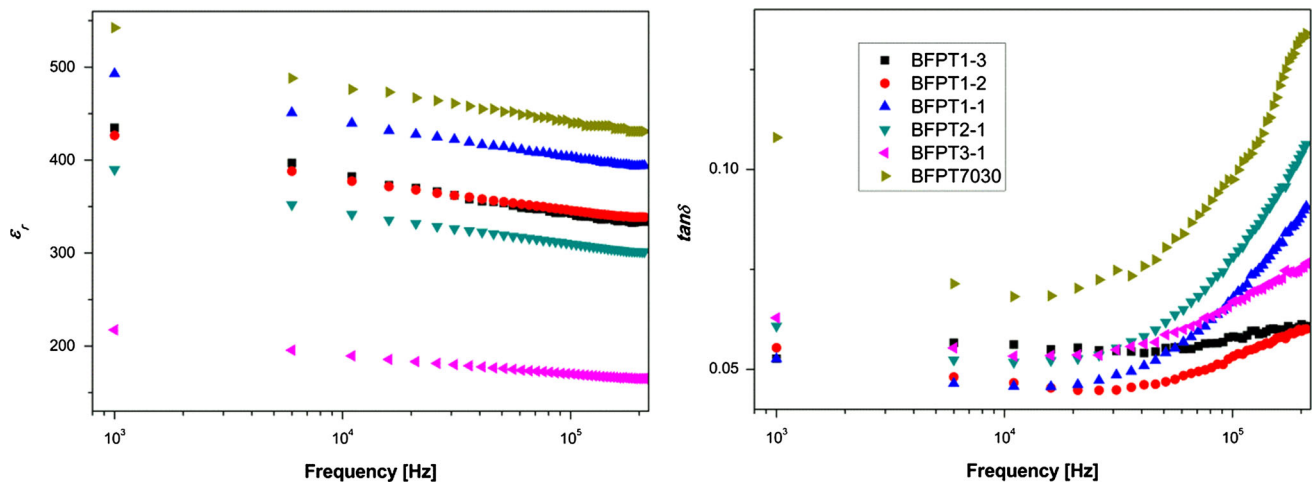


Fig. 6 Dielectric constant and loss tangent as function of frequency of BFPT1-1, BFPT1-2, BFPT1-3, BFPT2-1, BFPT3-1 and BFPT7030 thin films

BFPT1-2 is 0.05 at 1 kHz, smaller than that of other films. Furthermore, the loss tangent values for the film of BFPT1-2 are lower than that of other films at the frequency range from 1 to 100 kHz. Therefore, enhanced dielectric properties were found in BFPT1-2 thin film.

4 Conclusion

High-quality thin film of BFPT1-2 was prepared by sol–gel multilayer deposition method. XRD and SEM–EDS patterns showed that BFPT1-2 form a uniform solid solution film without any individual peaks of BF or PT, indicating that during the post-deposition heat treatment, BF and PT layer intermixed well with each other. And all the films showed highly (100) preferred orientation due to the induced orientation of LNO substrates. SEM fracture surface pictures indicate that more BF content, more thickness films were grown, which illustrate that BF would form more porous structure and leads to more thickness, and maybe this is the main reason for oxygen vacancies.

The electric properties test results showed obviously enhanced ferroelectric and dielectric properties in film of BFPT1-2. A saturated hysteresis loop measured at RT was found in BFPT1-2 with the highest P_r of 66 $\mu\text{C}/\text{cm}^2$ and a low E_c of 100 kV/cm, and also BFPT1-2 showed higher ϵ_r than other films except for BFPT1-1 and BFPT7030 thin film, and lowest $\tan\delta$ at the test frequency range of 1–100 kHz, indicating that with proper thickness and ratio of BF:PT, high-quality BFPT1-2 thin films can be prepared by sol–gel multilayer deposition method. And the RTA technique with heating rate of 1 $^\circ\text{C}/\text{s}$ also plays an important role for the improvement of ferroelectric and dielectric properties.

Acknowledgments The authors would like to acknowledge the financial support of Scientific Set Sail Project of Southwest Petroleum University (2014QHZ022) and Open Fund of Oil and Gas Material Key Laboratory (x151514kcl03).

References

- Kamba S, Nuzhnyy D (2007) Infrared and terahertz studies of polar phonons and magnetodielectric effect in multiferroic BiFeO_3 ceramics. *Phys Rev B* 75:024403
- Wang J, Neaton JB (2003) Epitaxial BiFeO_3 multiferroic thin film heterostructures. *Science* 299:1719–1722
- Kubel F, Schmid H (1990) Structure of ferroelectric and ferroelastic monodomain crystal of the perovskite BiFeO_3 . *Acta Crystall Sec B* 46:698–702
- Neaton JB, Ederer C (2005) First-principles study of spontaneous polarization in multiferroic BiFeO_3 . *Phys Rev B* 71:014113
- Woo-Hee K, Sung MY (2014) Ferroelectric domain wall motion in epitaxial PbTiO_3 and BiFeO_3 thin films. *Mater Lett* 124:47–49
- Levin I, Krayzman V (2014) Local structure underlying anomalous tetragonal distortions in BiFeO_3 – PbTiO_3 ferroelectrics. *Appl Phys Lett* 104:242913
- González-Vázquez OE, Íñiguez J (2009) Pressure-induced structural, electronic, and magnetic effects in BiFeO_3 . *Phys Rev B* 79:064102
- Liu HR, Liu ZL (2007) Improved electric properties in BiFeO_3 films by the doping of Ti. *J Sol-Gel Sci Technol* 41:123–128
- Pipinyas P, Rimeika A (2010) Analysis of leakage current mechanisms in BiFeO_3 thin films. *Ferroelectrics* 396:60–66
- Sun W, Li JF (2015) Phase transition and piezoelectricity of sol-gel processed Sm-doped BiFeO_3 thin films on Pt(111)/Ti/SiO₂/Si substrates. *J Mater Chem C* 3:2115–2122
- Singh SK, Shanthi S (2010) Reduced leakage current in BiFeO_3 – BiCrO_3 nanocomposite films formed by chemical solution deposition. *J Appl Phys* 108:054102
- Ueda K, Tabata H (1999) Coexistence of ferroelectricity and ferromagnetism in BiFeO_3 – BaTiO_3 thin films at room temperature. *Appl Phys Lett* 75:555–557

13. Chen L, Ren W (2010) Improved dielectric and ferroelectric properties in Ti-doped $\text{BiFeO}_3\text{-PbTiO}_3$ thin films prepared by pulsed laser deposition. *Thin Solid Films* 518:1637–1640
14. Sunder VVSS, Halliyal A (1995) Investigation of tetragonal distortion in the $\text{PbTiO}_3\text{-BiFeO}_3$ system by high-temperature X-ray diffraction. *J Mater Res* 10:1301–1306
15. Freitas VF, Cótica LF (2011) Synthesis and multiferroism in mechanically processed $\text{BiFeO}_3\text{-PbTiO}_3$ ceramics. *J Eur Ceram Soc* 31:2965–2973
16. Zhu WM, Guo HY (2008) Structural and magnetic characterization of multiferroic $(\text{BiFeO}_3)_{1-x}(\text{PbTiO}_3)_x$ solid solutions. *Phys Rev B* 78:014401
17. Amorín H, Correás C (2014) Multiferroism and enhancement of material properties across the morphotropic phase boundary of $\text{BiFeO}_3\text{-PbTiO}_3$. *J Appl Phys* 115:104104
18. Kothai V, Prasath Babu R (2013) Metastable morphotropic phase boundary state in the multiferroic $\text{BiFeO}_3\text{-PbTiO}_3$. *J Appl Phys* 114:114102
19. Siddaramanna A, Kothai V (2014) Stabilization of metastable tetragonal phase in a rhombohedral magnetoelectric multiferroic $\text{BiFeO}_3\text{-PbTiO}_3$. *J Phys D Appl Phys* 47:045004
20. Amorín H, Correás C (2012) Very high remnant polarization and phase-change electromechanical response of $\text{BiFeO}_3\text{-PbTiO}_3$ at the multiferroic morphotropic phase boundary. *Appl Phys Lett* 101:172908
21. Gupta S, Garg A (2009) Structural changes and ferroelectric properties of $\text{BiFeO}_3\text{-PbTiO}_3$ thin films grown via a chemical multilayer deposition method. *J Appl Phys* 105:014101
22. Gupta S, Bhattacharjee S (2011) Absence of morphotropic phase boundary effects in $\text{BiFeO}_3\text{-PbTiO}_3$ thin films grown via a chemical multilayer deposition method. *Appl Phys A* 104:395–400
23. Sakamoto W, Iwata A (2008) Ferroelectric properties of chemically synthesized perovskite $\text{BiFeO}_3\text{-PbTiO}_3$ thin films. *J Appl Phys* 104:104106
24. Khan MA, Comyn TP (2007) Large remanent polarization in ferroelectric $\text{BiFeO}_3\text{-PbTiO}_3$ thin films on Pt/Si substrates. *Appl Phys Lett* 91:032901
25. Esat F, Comyn TP (2014) Microstructure development of $\text{BiFeO}_3\text{-PbTiO}_3$ films deposited by pulsed laser deposition on platinum substrates. *Acta Mater* 66:44–53
26. Sakamoto W, Iwata A (2009) Electrical and magnetic properties of Mn-doped $0.7\text{BiFeO}_3\text{-}0.3\text{PbTiO}_3$ thin films prepared under various heating atmospheres. *Mater Chem Phys* 116:536–541
27. Li HM, Zhou YY (2010) Influence of heating rate on the crystalline properties of $0.7\text{BiFeO}_3\text{-}0.3\text{PbTiO}_3$ thin films prepared by sol–gel process. *Appl Sur Sci* 257:1407–1412
28. Gong W, Li JF (2004) Texture-control of sol–gel derived $\text{Pb}(\text{Mg}1/3\text{Nb}2/3)\text{O}_3\text{-PbTiO}_3$ thin films using seeding layer. *J Am Ceram Soc* 87(6):1031–1034
29. Gong W, Li JF (2004) Preparation and characterization of sol–gel derived (100) textured $\text{Pb}(\text{Zr}, \text{Ti})\text{O}_3$ thin films: PbO seeding role in the formation of preferential orientation. *Acta Mater* 52:2787–2793
30. Wu JG, Wang J (2009) Orientation dependence of ferroelectric behavior of BiFeO_3 thin films. *J Appl Phys* 106(10):104111
31. Liu HR, Liu ZL (2006) Electric and magnetic properties of multiferroic $(\text{BiFeO}_3)_{1-x}(\text{PbTiO}_3)_x$ thin films prepared by the sol–gel process. *J Phys D Appl Phys* 39:1022–1027
32. Khan MA, Comyn TP (2008) Growth and characterization of tetragonal bismuth ferrite-lead titanate thin films. *Acta Mater* 56:2110–2118
33. Zhu WM, Ye ZG (2006) Improved dielectric and ferroelectric properties of high Curie temperature $(1-x)\text{BiFeO}_3\text{-}x\text{PbTiO}_3$ ceramics by aliovalent ionic substitution. *Appl Phys Lett* 89:232904